

# Preparation of hydrophilic molecularly imprinted polymers via bulk polymerization combined with hydrolysis of ester groups for selective recognition of iridoid glycosides

Wenhua Ji<sup>1</sup> · Mingming Zhang<sup>2</sup> · Qianshan Gao<sup>1</sup> · Li Cui<sup>1</sup> · Lizong Chen<sup>1</sup> · Xiao Wang<sup>1,2</sup>

Received: 28 January 2016 / Revised: 4 May 2016 / Accepted: 10 May 2016 / Published online: 21 May 2016  
© Springer-Verlag Berlin Heidelberg 2016

**Abstract** Hydrophilic molecularly imprinted polymers (H-MIP) with molecular recognition ability for iridoid glycosides (IGs) have been obtained via bulk polymerization combined with hydrolysis of ester groups. H-MIP were characterized by Fourier transform infrared spectroscopy (FT-IR). The hydrophilicity was measured by the contact angle measurement and the water dispersion stability. The obtained H-MIP demonstrated high selectivity and specific binding ability to five IGs in aqueous media. The group extraction efficiency of molecular imprinted solid-phase extraction (MISPE) for five IGs was investigated, including loading sample, breakthrough volume, washing solvent, and elution solvent. Compared with non-imprinted solid-phase extraction (NISPE), the higher average recovery (95.5 %) of five IGs with lower relative standard deviations values (below 6.1 %) using MISPE combined with high-performance liquid chromatography (HPLC) were achieved at three spiked levels in three blank samples. Under the optimum MISPE conditions, the wide linear range with the correlation coefficient of  $R^2 \geq 0.9950$  for five IGs with low limits of detection (LOD) and quantification (LOQ) (0.01–0.08 and 0.03–0.27  $\mu\text{g mL}^{-1}$ , respectively) were obtained. Chromatograms obtained using MISPE columns demonstrated that the matrix interference has been minimized and great interferences around IGs

were also eliminated efficiently. These results indicated that the developed MISPE-HPLC method was selective, accurate, and applicable for the determination of IGs in water media.

**Keywords** Molecularly imprinted polymers · HPLC · Natural products · Solid phase extraction · Iridoid glycosides

## Introduction

Molecularly imprinted polymers (MIPs) are man-made receptors with specificity and high affinity towards the targeted analytes and analogous molecules [1–5]. Due to their capability of specific molecular recognition, MIPs have long been recognized as promising alternatives to biological receptors [6–8]. However, the presently developed MIPs targeting organic molecules are usually only organic solvent-compatible and normally show non-specific template binding in the aqueous media, which significantly limits their applications in many fields such as biomimetic sensors and immunoassay [9–11]. Hydrophilic MIPs (H-MIP) have been developed by using controlled/“living” radical precipitation polymerization technique (CRPP) [12, 13], hydrophilic monomers [14–17], and surface modification [18, 19]. Despite their excellent performance, the CRPP and surface modification referred to complicated preparation processes. Imprinting of hydrophilic compounds such as water-soluble glycosides is still challenge in molecular imprinting although hydrophilic monomers are a way to solve the problem. Few types of hydrophilic monomers limit the practical applications.

In our previous work, we prepared hydrophobic MIPs and superhydrophilic MIPs using 2,3,4,6-tetra-*O*-acetylglucopyranoside (TAGL) and alkenyl glycosides glucose (AGG) as functional monomers via the bulk polymerization, respectively [20, 21]. Both two kinds of MIPs possess highly selective imprinting cavities for recognizing gastrodin (GAS) in

**Electronic supplementary material** The online version of this article (doi:10.1007/s00216-016-9625-6) contains supplementary material, which is available to authorized users.

✉ Xiao Wang  
wangx@sdas.org

- <sup>1</sup> Shandong Key Laboratory of TCM Quality Control Technology, Shandong Analysis and Test Center, Shandong Academy of Sciences, 19 Keyuan Street, Jinan 250014, China
- <sup>2</sup> School of Life Sciences, Shandong Normal University, 88 Wenhua East Road, Jinan 250014, China

aqueous media. However, both MIPs suffer from significant disadvantages in the practical application process. MIPs/TAGL-SPE can be fouled easily and show an obvious decline when recycled, mainly due to the hydrophobic property and poor permeability. MIPs/AGG-SPE displays excellent superhydrophilicity. However, there would be a disadvantage of sorbents “dissolution-leakage” along with the eluent, which may cause the HPLC pipe block even treated with the centrifugation and filter membranes. Therefore, it is of tremendous interest to allow the good compromise between permeability and hydrophilicity.

Iridoid glycosides (IGs) are a family of hydrophilic compounds with extensive physiological activities extracted from the traditional Chinese herbal medicine [22, 23]. Due to excellent pharmacological properties of IGs, many quality control standards for original herbs and herbal preparations have been described in pharmacopoeias. For example, the minimal content of gardenoside (GDS) in *Gardenia Fructus* (the traditional medicines, *Zhi-zi* in Chinese) and *Zhizi Jinhua Pills* (*ZJP*; the famous Chinese traditional formulae) are 15 and 2.8 mg g<sup>-1</sup> defined by the Chinese Pharmacopoeia, respectively [24, 25]. IGs analyses have been developed using high-performance liquid chromatography (HPLC) techniques [26–32]. However, due to the complexity of traditional Chinese medicines (TCMs) matrices in the hydrophilic media, it is necessary to enrich the target compounds before detecting for HPLC analysis. Moreover, the single active ingredient is less reasonable than using multi-component quantification in TCMs quality control. It is significant for the targeted enrichment of structurally similar IGs in very complicated matrixes.

Herein, we report an efficient synthesis of H-MIP for families of IGs via bulk polymerization combined with hydrolysis of ester groups using TAGL as functional monomers. Loganin (LOG), a cheap and accessible IG, has been prepared from fruits of *Cornus officinalis* in our laboratory and was chosen as the dummy template. This compound could also circumvent the deficiency associated with template leakage in the consequent analysis by HPLC. Its structural skeletons resemblance with IGs could enable the production of a group-selective MIPs. *N,N'*-methylene diacrylamide (MBA), ethyleneglycol dimethacrylate (EGDMA), and divinylbenzene (DVB) were used as cross-linkers. In the present study, molecular imprinted solid-phase extraction (MISPE), an effective sample pre-treatment method, was established for the enrichment of five marker IGs. Then, MISPE coupled with HPLC was developed and validated for simultaneous determination of five IGs in *Gardenia Fructus*.

## Experimental

### Reagents and chemicals

Loganin (LOG), geniposide (GPS), gardenoside (GDS), genipin-1-*O*-gentiobioside (GGB), *shanzhiside* methylester

(SAM), and geniposidic acid (GPA) were obtained from Yiyao Bio-tech Co., Ltd. (Shanghai, China). Genipin (GEP) and arbutin (ARB) were purchased from Aladdin Bio-tech Co., Ltd. (Shanghai, China). HPLC-grade reagents were from Fisher Scientific (Fair Lawn, NJ, USA). 2,2-azoisobutyronitrile (AIBN; initiator), *N,N'*-methylene diacrylamide (MBA; cross-linker), divinylbenzene (DVB; cross-linker), ethylene glycol dimethacrylate (EGDMA; cross-linker), dimethylsulfoxide (DMSO; porogen), and sodium methoxide (NaOMe) were purchased from Xiya chemistry Co. Ltd (Chengdu, China). Conventional SPE (SampliQ C18, SampliQ Silica, SampliQ PS-DVB, and SampliQ Alumina N) were purchased from Agilent (Santa Clara, CA, USA). Chemical structures of investigated compounds are shown in Fig. 1.

### Typical synthesis of polymers

A typical experimental procedure for bulk polymerization combined with hydrolysis of ester groups is described below: LOG (0.5 mmol) and TAGL (5 mmol) were added in DMSO (5 mL) in a reaction bulb followed by 5 mg of the initiator AIBN and crosslinker MBA (10 mmol). The polymerization solutions were thermo-polymerized in protection of nitrogen for 24 h at 60 °C. After smashed, the polymers were sieved through the 45–55 µm sieves. The obtained particles were dispersed in NaOMe/MeOH (5 mmol in 50 mL) for refluxing 6 h to remove templates and hydrolyze ester groups. H-MIP were washed with methanol until neutral; 4.02 g polymer particles were obtained (64.9 % yield) after dried overnight under vacuum at 60 °C.

Hydrophilic non-imprinted polymers (H-NIP) were prepared without introduction of templates.

### Characterization of polymers

Rise-1010 surface area measurement (Jinan, China) was used to determine nitrogen adsorption-desorption isotherms. The total pore volume and specific surface area were calculated by the Brunauer-Emmett-Teller (BET) method. Fourier transform infrared spectroscopy (FT-IR) and scanning electron microscopy images (SEM) were obtained with Nicolet710 (Foster City, CA, USA) and SWPRATM55 (Carl Zeiss, AG, Aalen, Germany), respectively.

### HPLC analysis

The samples were analyzed by the Agilent Series 1120 system (Agilent Technologies, Palo Alto, CA, USA) equipped with an YMC-Pack ODS-A (5 µm, 4.6 × 250 mm) analytical column. The chromatographic data was controlled by the software of *Chemstation B0403*. The mobile phase for HPLC analysis was acetonitrile/H<sub>2</sub>O (10:90, v/v) at 30 °C. The flow rate and the injection volume were 1.0 mL min<sup>-1</sup> and 10 µL, respectively. All analytes were detected at 238 nm.

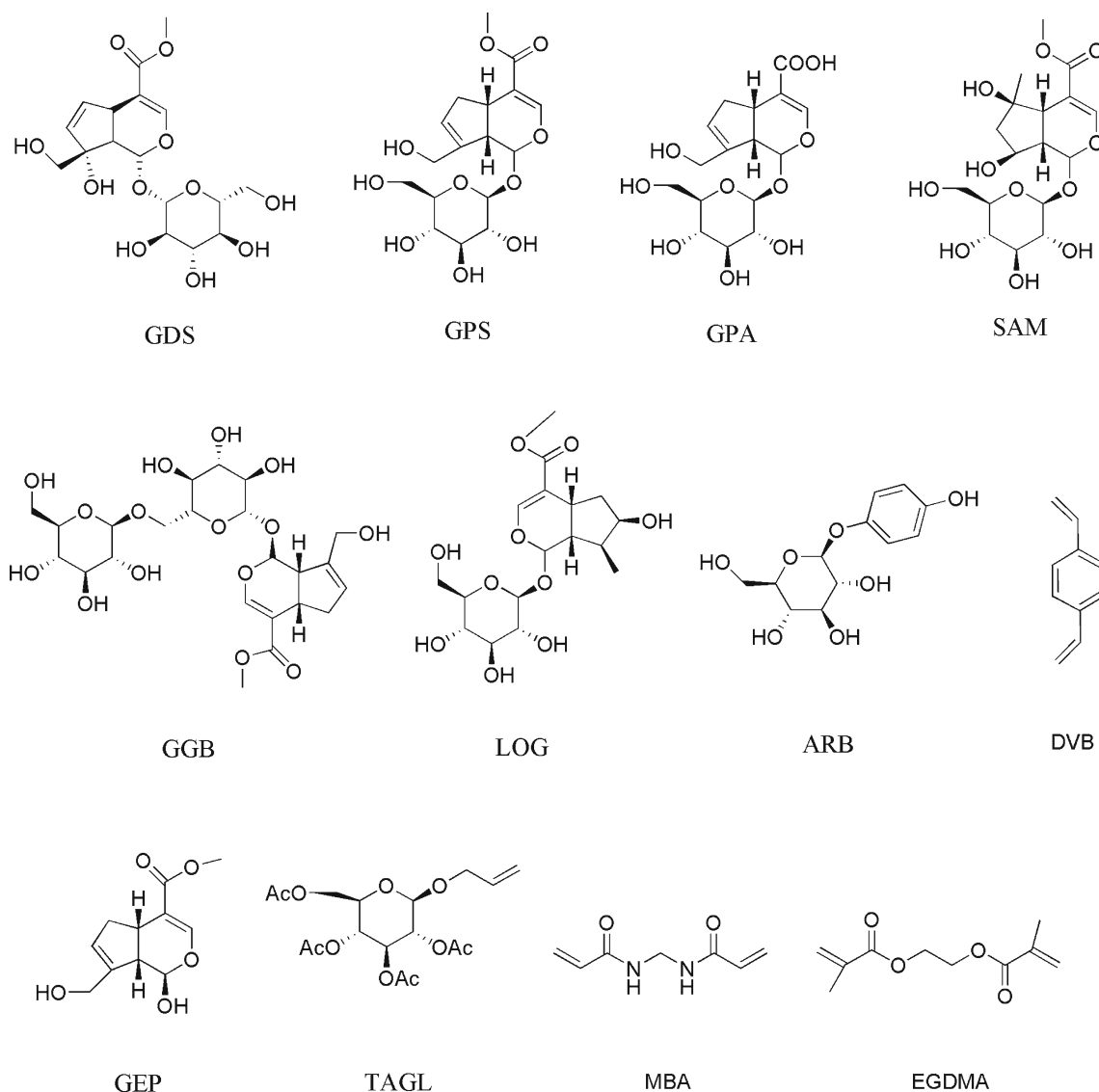


**Fig. 1** Chemical structures of investigated compounds

### Measurement of the static water contact angles

Polymers were dispersed ultrasonically in DMF ( $10 \text{ mg mL}^{-1}$ ), and the films were carried out by casting the suspension solutions onto the glass surfaces. The solvent was evaporated under vacuum and then the resulting films were dried at  $25 \text{ }^\circ\text{C}$  for 12 h. The static water contact angles were determined by using an OCA40 video optical contact angle equipment (Dataphysics, Germany).

### Adsorption experiments

Adsorption experiments were carried out according to the literature with a minor modification [21, 33]. The details are as follows:

**Static adsorption** GDS was chosen as the model compound; 10 mg polymers were mixed with 2.5 mL various concentrations of GDS ( $0.05\text{--}0.8 \text{ mmol L}^{-1}$ ). After being shaken for 150 min at  $25 \text{ }^\circ\text{C}$ , the sorbents were isolated by centrifugation. The supernatant solution was analyzed by HPLC. The equilibrium adsorption capacity ( $Q_e$ ,  $\text{mmol g}^{-1}$ ) was calculated according to the equation [34]:

$$Q_e = (C_i - C_e)v/m$$

where  $C_e$  ( $\text{mmol L}^{-1}$ ) and  $C_i$  ( $\text{mmol L}^{-1}$ ) are the equilibrium and initial concentrations of GDS.  $v$  (mL) is the volume of solution, and  $m$  (mg) is the mass of sorbents.

**Scatchard analysis** The Scatchard equation was employed to evaluate the relation between the binding

ability and concentration, and the equation is expressed as [35]:

$$Q_e / C_e = (Q_{\max} - Q_e) / K_d$$

where  $Q_e$  stands for the equilibrium binding capacity ( $\text{mmol g}^{-1}$ ) of GDS onto H-MIP,  $K_d$  represents the equilibrium dissociation constant ( $\text{mmol L}^{-1}$ ),  $Q_{\max}$  ( $\text{mmol g}^{-1}$ ) is the theoretical maximum adsorption amount of GDS onto the H-MIP, and  $C_e$  ( $\text{mmol L}^{-1}$ ) is the equilibrium concentration of GDS in the solution.

**Kinetic adsorption** The kinetic adsorption experiment was investigated with 10 mg polymers and the standard solutions of GDS (2.5 mL,  $0.3 \text{ mmol L}^{-1}$ ). The solution was shaken at regular time intervals, and the equilibrium concentration was measured by HPLC.

### Selectivity experiment

Selectivity study was evaluated with five IGs and two analogs including GEP and ARB; 7.0 mL of the standard solution of each analyte at the initial concentration of  $0.3 \text{ mmol L}^{-1}$  was shaken with 10 mg sorbents for 120 min. The equilibrium concentration was measured by HPLC.

### MISPE conditions

The 500 mg of H-MIPs and H-NIPs were packed into an empty SPE column (5 mL). The polymers were rinsed with pure water and then with the loading solvent. Each five IGs was dissolved in loading solvent to final concentration of  $0.5 \mu\text{g mL}^{-1}$ . After loading through columns, washing solvent was passed. Finally, the elution step was performed to completely extract IGs. The loading, washing, and eluting fractions were analyzed by HPLC to detect IGs concentration.

The MISPE protocol was optimized as follows:

Flow rate at 1.0 to  $6.0 \text{ mL min}^{-1}$ ; loading solvent includes pH from 3.0 to 12.0 spiked with sodium hydroxide or dilute hydrochloric acid; breakthrough volume at 50 to 200 mL; washing solvent includes methanol, tetrahydrofuran, acetonitrile, acetone, and methanol- $\text{H}_2\text{O}$  (10:1, v/v); volumes of washing solvent at 2.0 to 10.0 mL; elution solvent includes EtOH/Et<sub>3</sub>N (95:5, v/v), EtOH/Et<sub>3</sub>N (90:10, v/v), and EtOH/Et<sub>3</sub>N (85:15, v/v); and volumes of elution solvent at 3 to 9.0 mL.

### Sample preparation and application of MISPE to samples

*Gardenia Fructus* powder was accurately weighed to 0.1 g in a stoppered conical flask; 50.0 mL of water was added. The

mixture was extracted with ultrasonic at 25 °C for 30 min. The supernatant was filtered through a 0.45- $\mu\text{m}$  PTFE membrane, and the mixture was accurately diluted with water to 100 mL and mixed well for further adsorption experiment.

MIPs (500 mg) were packed into an empty SPE column (5 mL). After adjustment with 10 mL water, 100 mL of the loading sample was flowed through the MISPE column at the constant flow rate of  $6.0 \text{ mL min}^{-1}$ . The column was washed and eluted with 6 mL of acetonitrile and 3 mL of EtOH/Et<sub>3</sub>N (85:15, v/v), respectively. The elution product was analyzed by HPLC.

## Results and discussion

### H-MIP synthesis and characterization

In this study, LOG was chosen as the dummy template by considering the special structural skeletons of IGs. MBA, EGDMA, and DVB were used as cross-linkers, respectively. A molar ratio of 1:2:4 for template, functional monomer, and cross-linker was applied as the previously reported [18].

In order to confirm the hydrolysis of functional groups, the obtained H-MIP were characterized by infrared spectroscopy (IR). As shown in Fig. S1, the H-MIP displayed the characteristic peaks of the hydroxyl groups of O-H at the range of  $3400\text{--}3600 \text{ cm}^{-1}$  compared with the infrared data of the non-hydrolytic MIP. It must be noted that the C=O stretching vibration band of MIP/OH-DVB is still present close to  $1600\text{--}1700 \text{ cm}^{-1}$  (Fig. S1d). These results indicated that hydrophobic ester groups had been partially hydrolyzed to become hydrophilic hydroxy groups and partial imprinted cavities were still retained. The molecular imprinted technology requires the shape and functional group of imprinted cavities match with the template. In this work, the generated cavities in MIPs match the template. Even though after hydrolysis of TAGL, the residual imprinted cavities can specifically recognize the template and structural analogs.

Contact angle measurement is an important tool to evaluate the extent of hydrophilicity [36]. As shown in Fig. S2A, the static water contact angle of MIP<sub>MBA</sub>, MIP<sub>EGDMA</sub>, and MIP<sub>DVB</sub> were nearly 130°, 135°, and 145°, respectively. In sharp contrast, the static water contact angle of H-MIP<sub>MBA</sub>, H-MIP<sub>EGDMA</sub>, and H-MIP<sub>DVB</sub> were nearly 40°, 45°, and 56°, respectively. The contact angles of H-MIP decreased compared with these of MIP. H-MIP<sub>MBA</sub> exhibited the smallest water contact angle which might be caused by the better hydrophilicity of MBA. The relatively high hydrophilic property of H-MIP suggested that the inner structures have been modified. In addition, the dispersion properties of the H-MIP and MIP in pure water were investigated. After the ultrasonic dispersion in pure water ( $10 \text{ mg mL}^{-1}$ ) at 25 °C, the dispersed mixtures were allowed to stand for different times. The typical photographs of the resultant solutions were showed in Fig. S2B, from which it can be seen clearly that there was

much slower sedimentation for H-MIP in comparison with MIP. These results confirmed that H-MIP obtained via bulk polymerization combined with hydrolysis of ester groups displayed excellent hydrophilicity and the specific separation application can be focused on.

Surface area analysis performed through BET nitrogen adsorption-desorption measurements revealed further differences in the structures of three kinds of polymers. As summarized in Table S1, non-hydrolytic MIPs prepared with the same cross-linker had no obvious difference in the surface area and total pore volume. However, hydrolytic MIPs owned the smaller surface area and significantly larger pore volume, mainly caused by the hydrolysis of ester groups.

The morphologies of MIPs/TAGL and hydrolytic MIPs/TAGL were shown in Fig. S3. No significant differences in particle shape and morphology were observed. This result indicated that imprinted cavities were still retained. Sorbents “dissolution-leakage” along with the eluent from MISPE/AGG columns may cause the HPLC pipe block. The SEM study revealed the dissolution-leakage feature of MISPE/AGG and hydrolytic MISPE/TAGL. It is to be seen that MIPs/AGG still existed in the eluent even treated with the filter membrane (0.25  $\mu\text{m}$ ) for twice (Fig. S4A), mainly due to the excellent superhydrophilicity. In sharp contrast, there was little dissolution-leakage from hydrolytic MISPE/TAGL columns (Fig. S4B). Compared with the superhydrophilicity of MIPs/AGG, the moderate hydrophilicity of hydrolytic MIPs/TAGL can avoid the sorbents dissolution-leakage and hydrolytic MIPs are more favorable to SPE-HPLC.

### Selectivity study of H-MIP

*Gardenia* Fructus consist of five typical IGs including GDS, GPS, GPA, GGB, and SAM. To evaluate the applicability of “bulk polymerization combined with hydrolysis of ester groups” as suitable tools to prepare H-MIP, the selective adsorption of H-MIP with different cross-linker has been investigated by measuring the competitive adsorptive capacities towards five IGs and another two analogs, ARB and GEP. As can be seen from Fig. 2, H-MIP exhibited higher IF value ( $Q_{e, \text{H-MIP}}/Q_{e, \text{H-NIP}} > 2.0$ ) for four IGs. What is noteworthy is that the low IF value was obtained for GGB, which may be due to the fact that molecular skeleton of GGB is slightly different from that of LOG. However, the lower IF values were obtained for ARB and GEP. These results clearly confirmed that the binding sites in H-MIP had non-specific adsorption for analogs which own entirely different molecular structure compared with LOG.

### Binding properties of H-MIP and H-NIP

We performed the classical steady-state binding experiments by using H-MIP<sub>MBA</sub>/GDS as a model in the aqueous media. As

shown in Fig. 3a, the amount of GDS binding to the polymers increased along with its initial concentration and the saturation binding was observed with the initial concentration of 0.7  $\text{mmol L}^{-1}$ . H-MIP<sub>MBA</sub> had higher affinity for GDS than H-NIP<sub>MBA</sub>, MIP<sub>MBA</sub>, and NIP<sub>MBA</sub>. The obviously higher adsorption capacity of H-MIP can be due to the excellent hydrophilicity and the presence of specific binding sites which were not destroyed during hydrolyzing. As showed in Fig. 3b, the Scatchard plot of the H-MIP<sub>MBA</sub> isotherm shows two straight lines, indicated that the heterogeneous binding sites in H-MIP could be classified into two typical groups: one that represents the binding sites with higher affinity ( $Q_{\text{max}}=0.39 \text{ mmol g}^{-1}$  and  $K_d=0.040 \text{ mmol L}^{-1}$  for H-MIP<sub>MBA</sub> high) and another with lower affinity ( $Q_{\text{max}}=2.05 \text{ mmol g}^{-1}$  and  $K_d=0.52 \text{ mmol L}^{-1}$  for H-MIP<sub>MBA</sub> low) [37]. The low selective binding spots are present in bigger amount and have a higher dissociation rate than the high-selective sites. The H-NIP<sub>MBA</sub> curve demonstrates a linear slope ( $Q_{\text{max}}=0.28 \text{ mmol g}^{-1}$  and  $K_d=0.085 \text{ mmol L}^{-1}$  for H-NIP<sub>MBA</sub>), which indicates one type of homogeneous binding sites possessing low selectivity. The overall binding affinity of H-MIP<sub>MBA</sub> towards GDS is higher than compared with H-NIP<sub>MBA</sub>.

The kinetic adsorption curves of GDS onto polymers are shown in Fig. 4. It can be clearly seen that the adsorption equilibrium could be achieved quickly within 10 min, while it cannot reach equilibrium in more than 120 min for H-NIP<sub>MBA</sub>. The rapid and preferential adsorption of analytes onto the recognition sites might lead to the higher adsorption rate of H-MIP<sub>MBA</sub>.

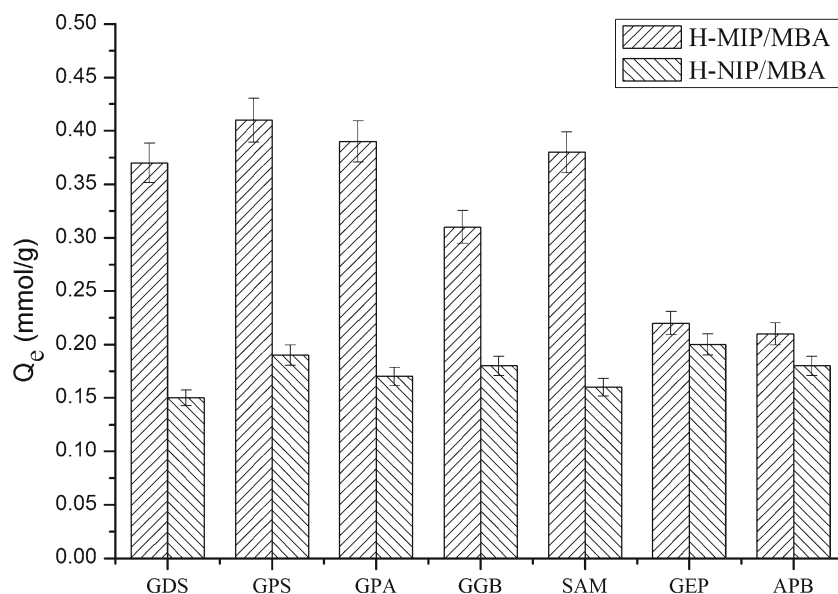
### Optimization of MISPE parameters

As the artificial material, MIPs own selective recognizing cavities for specifically binding the template compound or structurally related compounds. Five typical IGs including GPS, GDS, GPA, GGB, and SAM share the similar chemical structure composed of monoterpene with a glucose moiety. Therefore, we investigated the group extraction efficiency of MISPE for five IGs by optimizing the conditions including loading sample, breakthrough volume, washing solvent, and elution solvent.

#### Optimized of loading sample

The sample loading pH can obviously affect the adsorption capacity during the SPE process. As shown in Fig. 5, the recoveries of five IGs were all below 70 % at pH from 3.0 to 6.0, mainly due to the hydrolysis of glycosidic bonds in the acidic condition. With the sample pH increasing from 7.0 to 12.0, the recoveries of five IGs decreased steadily, especially for GAP. This might be mainly related to the dissociation constants ( $\text{p}K_a$ ). The  $\text{p}K_a$  values of five IGs were  $12.80 \pm 0.70$  (GPS),  $12.28 \pm 0.60$  (GDS),  $4.49 \pm 0.60$  (GPA),  $12.80 \pm 0.70$  (GGB), and  $12.78 \pm 0.70$  (SAM) as calculated using the SciFinder Scholar database [38]. The low recoveries at

**Fig. 2** The specific binding behaviors of H-MIP and H-NIP for five IGs and two analogs. Error bars represent 1 standard deviation for three measurements



pH=12.0 should be likely due to undergo the ionization to become the organic salts. After that, the imprinting interactions between analytes and sorbents were decreased by the change of the 3D structures of IGs. Therefore, pH from 7.0 to 8.0 was selected for subsequent works.

The effect of loading flow rate on IGs recoveries was then studied. Recoveries ranging from 93.1 to 98.3 % (RSD <5.0 %,  $n=3$ ) were obtained up to the flow rate of  $6.0 \text{ mL min}^{-1}$ . Thus, the value of  $6.0 \text{ mL min}^{-1}$  was chosen in further research.

#### Breakthrough volume

The breakthrough volume of MISPE columns was investigated by percolating various volumes of samples (50, 100, 150, and 200 mL). IGs average recoveries were 98.2, 94.1, 90.2, and 70.4 %, respectively. The result indicated that the loss of

IGs was below 10 % when the loading volume was increased to 150 mL. However, the recoveries of IGs only reached about 70 % at the loading volume of 200 mL. To guarantee the development of a practical analytical approach and the recoveries of IGs, a volume of 100 mL was selected to increase the sensitivity of the developed HPLC method.

#### Optimized of elution solvent

The elution solvent was performed to remove the binding gingerols as much as possible. Thus, 100 mL solutions were loaded through the MISPE column and then eluted with 9 mL of elution solvent (3+3+3 mL). Each 3 mL fraction was analyzed by HPLC to determine the recoveries of five IGs. As shown in Fig. 6, the quantitative recovery of five IGs (98 %, 5 % RSD,  $n=3$ ) was obtained through using 9 mL of EtOH/Et<sub>3</sub>N (95:5, v/v). To reduce the volume, 3 mL of the

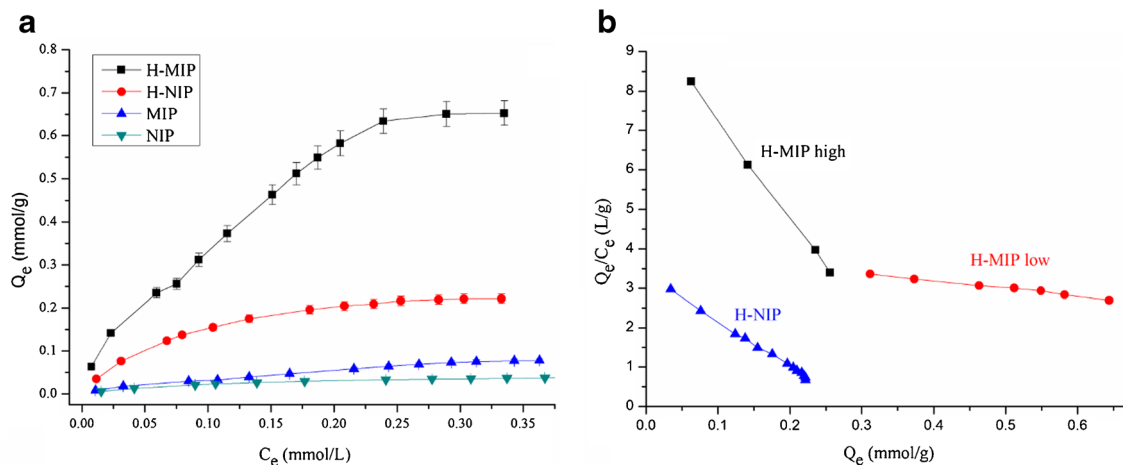


**Fig. 3** a Adsorption isotherms of polymers. b Scatchard analysis of H-MIP and H-NIP. Error bars represent one standard deviation for three measurements

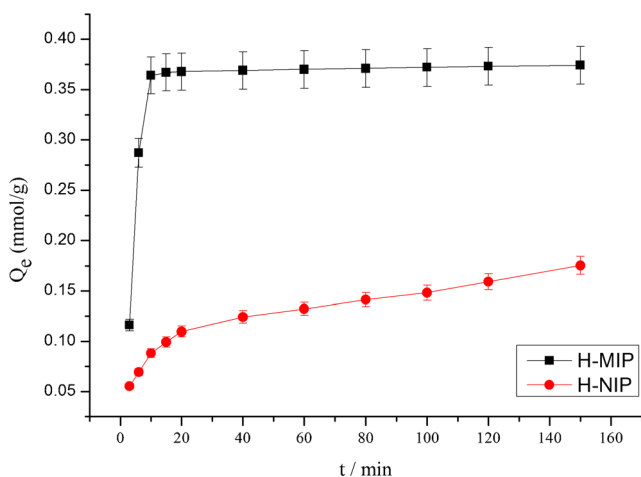


**Fig. 4** Dynamic adsorption of H-MIP and H-NIP. Error bars represent 1 standard deviation for three measurements

solution containing 15 % Et<sub>3</sub>N in EtOH was used. The interactions between sorbents and IGs were disrupted by the addition of Et<sub>3</sub>N. Therefore, 3 mL of EtOH/Et<sub>3</sub>N (85:15, v/v) was selected.

#### Optimized of washing solvent

The washing step, as a crucial procedure, needed to maximize the specific interactions and reduce non-specific interactions between sorbents and target analytes. After loading onto the column, 6.0 mL of methanol, tetrahydrofuran, acetonitrile, acetone, and methanol-H<sub>2</sub>O (10:1, v/v) as the washing solvent were investigated. After washing with 6.0 mL of acetonitrile, the recoveries of IGs from the MISPE column was above 90 %, whereas the recoveries of IGs from the NISPE column decreased to less than 70 %, as shown in Fig. 7. Methanol and methanol-H<sub>2</sub>O (10:1, v/v) were sufficient to remove IGs from the NISPE column, but most of IGs were also eluted from the

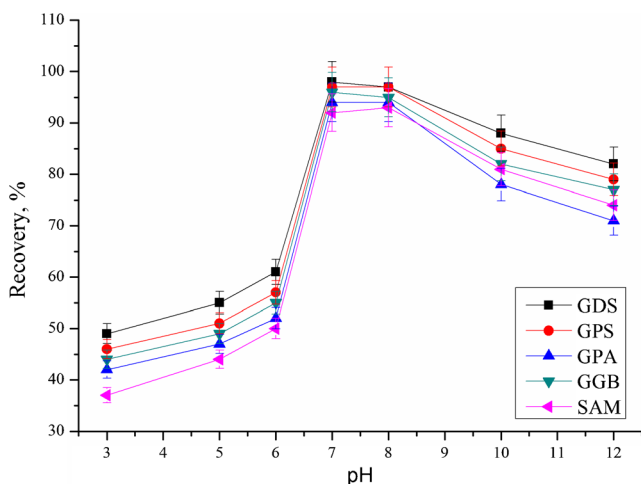


**Fig. 5** Effect of the loading sample pH on recoveries of IGs. Error bars represent one standard deviation for three measurements

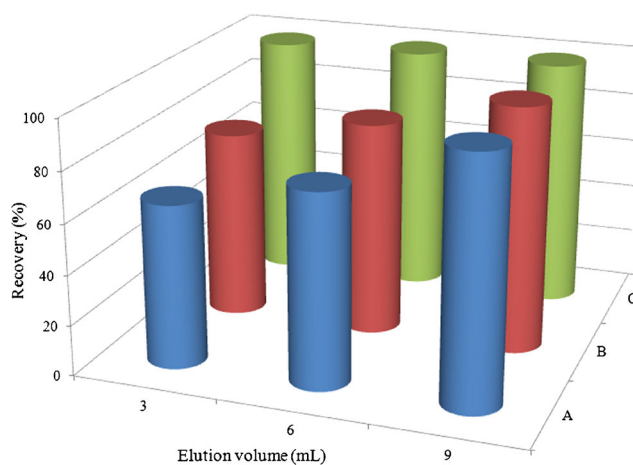


**Fig. 6** Effect of elution solvents: **A** EtOH/Et<sub>3</sub>N (95:5, v/v). **B** EtOH/Et<sub>3</sub>N (90:10, v/v). **C** EtOH/Et<sub>3</sub>N (85:15, v/v). Error bars represent 1 standard deviation for three measurements

MISPE column simultaneously. For choosing the optimal washing solution volume, different volumes of acetonitrile from 2.0 to 10.0 mL were investigated. The recoveries of IGs kept almost constant with the increasing volume from 2.0 to 6.0 mL, but then decreased with the volume from 6.0 to 10.0 mL. With the purification effect, 6 mL of acetonitrile was selected as washing solution in further studies.

#### Comparison of MISPE with conventional SPE

Recoveries of IGs by MISPE and conventional SPE (SampliQ C<sub>18</sub>, SampliQ Silica, SampliQ PS-DVB, and SampliQ Alumina N) were investigated. GDS was chosen as the model molecules. The lower recoveries for GDS were obtained from SampliQ C<sub>18</sub>, SampliQ Silica, SampliQ PS-DVB, and SampliQ Alumina N (below 70 %), mainly due to the non-special adsorption for GDS (Fig. S5). Compared with conventional SPE, MISPE columns indicated the higher recovery for

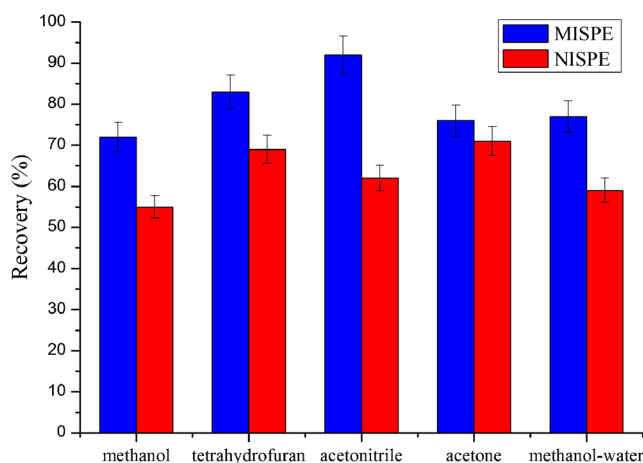


**Fig. 7** Effect of washing solvents on recoveries of IGs. Error bars represent 1 standard deviation for three measurements

**Table 1** MISPE-HPLC validation data

| IGs | Linearity range ( $\mu\text{g/mL}$ ) | $R^2$  | LOD ( $\mu\text{g/mL}$ ) | LOQ ( $\mu\text{g/mL}$ ) |
|-----|--------------------------------------|--------|--------------------------|--------------------------|
| GPS | 0.01–50                              | 0.9959 | 0.01                     | 0.03                     |
| GDS | 0.01–50                              | 0.9961 | 0.01                     | 0.03                     |
| GPA | 0.04–50                              | 0.9972 | 0.02                     | 0.07                     |
| SAM | 0.07–50                              | 0.9952 | 0.05                     | 0.19                     |
| GGB | 0.09–50                              | 0.9966 | 0.08                     | 0.27                     |

GDS (above 95 %). The high selectivity could be due to the molecular recognition of H-MIP to GDS.

#### The reusability of MISPE column

An excellent performance for sorbents is expected to utilize repeatedly. To evaluate the reusability of MISPE columns, adsorption-elution cycle was repeated 11 times by using the same sorbents. It could be seen from Fig S6 that the recoveries of IGs were above 90 % after eight cycles, but further reuse could result in obvious loss of recoveries for IGs. It may be caused by the jam for some imprinted sites during the regeneration of sorbents.

#### Method validation

In order to evaluate the proposed MISPE-HPLC method for the quantification of IGs in water media, the linearity was estimated by analyzing IGs standard solutions at various concentrations. The results are shown in Table 1. It can be seen

that excellent linearity was obtained ranging from 0.01 to 50  $\mu\text{g mL}^{-1}$  with the correlation coefficient of  $R^2 \geq 0.9950$ . The limit of detection (LOD) and limit of quantitation (LOQ) values were lower than the earlier reported works (Table S2), ranging between 0.01–0.08 and 0.03–0.27  $\mu\text{g mL}^{-1}$ , respectively.

To validate the developed method, the recoveries of IGs at different spiking levels in blank samples (0.4, 1.0, and 5.0  $\mu\text{g mL}^{-1}$ ) pre-treated with MISPE columns were determined and calculated. Blank samples which were all confirmed to lack detectable IGs were the extracting solution of *Coptis radix*, *Phellodendron stem*, and *Scutellaria radix*, respectively. As summarized in Table 2, the recoveries of IGs were in the range of 90.8 to 97.9 % with the relative standard deviation (RSD) values below 6.1 %. As can be seen from Table 2, the average recovery of MISPE method was 95.5 %, demonstrating that the pre-treated method had an excellent recovery. All these results indicated that the developed MISPE-HPLC method was selective, accurate, and applicable for the determination of IGs in water media.

#### Application of MISPE procedure in the real samples analysis

The practicability of MISPE-HPLC method has been further evaluated in the real samples analysis. Figure 8 showed the typical chromatograms. The chromatographic peaks of GPA, GGB, and SAM in 100 mL sample were unobvious due to the very low concentration without any pre-treatments. The chromatographic peaks of IGs could be found after 100 mL sample

**Table 2** Analysis of five IGs in different spiking levels using MISPE-HPLC

| IGs | Spiking level ( $\mu\text{g mL}^{-1}$ ) | <i>Coptis radix</i> |                  | <i>Phellodendron stem</i> |                  | <i>Scutellaria radix</i> |                  |
|-----|---|---------------------|------------------|---------------------------|------------------|--------------------------|------------------|
|     |   | Recovery (%)        | RSD (% $, n=3$ ) | Recovery (%)              | RSD (% $, n=3$ ) | Recovery (%)             | RSD (% $, n=3$ ) |
| GPS | 0.4                                     | 96.3                | 4.2              | 95.1                      | 3.4              | 97.3                     | 4.1              |
|     | 1.0                                     | 95.2                | 3.4              | 94.6                      | 5.5              | 97.1                     | 5.3              |
|     | 5.0                                     | 94.2                | 5.6              | 93.5                      | 4.4              | 96.3                     | 3.5              |
| GDS | 0.4                                     | 97.5                | 4.8              | 97.3                      | 3.4              | 96.1                     | 5.8              |
|     | 1.0                                     | 95.5                | 6.1              | 95.2                      | 3.6              | 95.4                     | 4.9              |
|     | 5.0                                     | 97.9                | 3.3              | 96.4                      | 4.7              | 97.1                     | 5.4              |
| GPA | 0.4                                     | 94.1                | 3.5              | 95.1                      | 5.1              | 93.8                     | 4.6              |
|     | 1.0                                     | 95.1                | 4.7              | 96.3                      | 5.5              | 94.9                     | 4.8              |
|     | 5.0                                     | 94.7                | 4.9              | 91.3                      | 4.6              | 92.4                     | 3.9              |
| SAM | 0.4                                     | 94.8                | 3.9              | 96.4                      | 4.7              | 97.4                     | 3.5              |
|     | 1.0                                     | 96.3                | 3.7              | 97.5                      | 4.8              | 95.3                     | 4.7              |
|     | 5.0                                     | 97.3                | 5.5              | 95.5                      | 3.9              | 96.5                     | 5.9              |
| GGB | 0.4                                     | 90.8                | 4.4              | 91.3                      | 4.6              | 92.6                     | 4.9              |
|     | 1.0                                     | 93.2                | 4.5              | 91.2                      | 5.5              | 90.8                     | 4.3              |
|     | 5.0                                     | 92.1                | 4.1              | 92.3                      | 4.3              | 90.5                     | 5.5              |



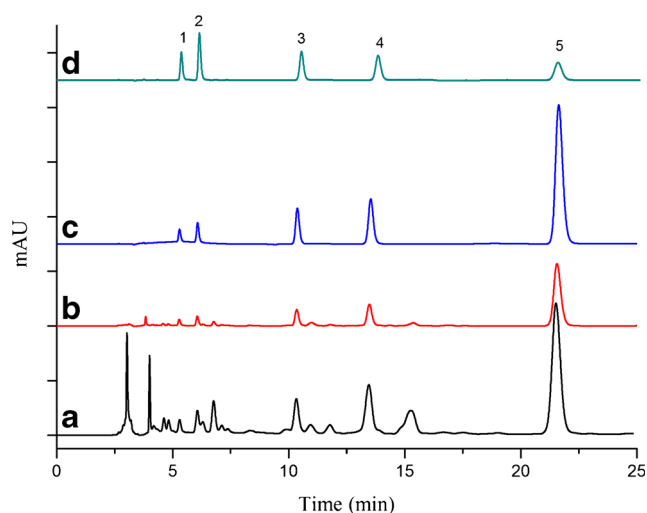


**Fig. 8** Chromatograms of *Gardenia Fructus* samples. *Gardenia Fructus* extracts with concentration (100.0 mL extracts were concentrated to 3.0 mL) (a); chromatogram of eluting solutions from NISPE column (b); chromatogram of eluting solutions from MISPE column (c); standards of five IGs (d). Peak identifications: 1, GPA; 2, GGB; 3, SAM; 4, GDS; 5, GPS

was concentrated to 3 mL. However, the matrix interference was also maximized and the impurity peaks were very obvious (Fig. 8a). The results implied that two methods, the direct injection and sample preconcentration, were not suitable for the *Gardenia Fructus* quality control. After selectively enriching IGs by using MISPE columns, the matrix interference has been minimized and great interferences around IGs were also eliminated efficiently (Fig. 8c). Although the chromatogram with clear peaks of IGs could be obtained through NISPE, the peaks obtained in NISPE are obviously lower than the peaks obtained in MISPE (Fig. 8b). Therefore, NISPE was not suitable for quantization due to the lower recovery. The concentrations of five IGs in five commercial samples of *Gardenia Fructus* have been determined by using the established quantitative method. From Table 3, GPS was analyzed with the highest concentration from five commercial samples, comparing with the smaller amount of GPA. All the results indicate that H-MIP prepared in this study own the imprinting recognition ability and the proposed MISPE-HPLC procedure can be applied to the enrichment and detection of IGs in the aqueous media.

**Table 3** Concentration (mg/g, RSD <5 %, n=3) of IGs in *Gardenia Fructus*

| Samples                            | GDS  | GPS  | GPA | SAM | GGB |
|------------------------------------|------|------|-----|-----|-----|
| <i>Gardenia Fructus</i> (Heibei)   | 15.8 | 21.5 | 1.1 | 4.2 | 3.1 |
| <i>Gardenia Fructus</i> (Fujian)   | 15.9 | 21.2 | 1.1 | 4.3 | 3.3 |
| <i>Gardenia Fructus</i> (Sichuan)  | 15.9 | 20.4 | 1.1 | 4.2 | 3.4 |
| <i>Gardenia Fructus</i> (Jiangxi)  | 16.8 | 22.3 | 1.1 | 4.4 | 3.6 |
| <i>Gardenia Fructus</i> (Zhejiang) | 15.4 | 22.9 | 1.1 | 3.1 | 3.8 |

## Conclusions

In conclusion, this study describes an innovative process for the preparation of hydrophilic molecularly imprinted polymers with excellent specific recognition ability for glycosides in aqueous media. H-MIP are synthesized by combining the bulk polymerization and the hydrolysis of ester groups. The infrared data of hydrolytic MIPs suggest that hydrophilic groups have been introduced into polymers. The hydrophilicity and water dispersion stability of H-MIP have been observably improved by the hydrolysis of polymers. The obtained H-MIP demonstrate high template selectivity and specific binding ability to five IGs. The presented MISPE-HPLC procedure can be applied to the selective enrichment and determination of IGs from the aqueous media. Based on our study, five IGs could be chosen as the marker compounds for the quality criteria for *Gardenia Fructus*, instead of only GDS being specified in the Chinese Pharmacopoeia. The multi-component quantification is the mainly improvement for the TCM quality control.

**Acknowledgments** This study was financially supported by the Natural Science Foundation of Shandong (ZR2015BQ005) and a research grant from Shandong Analysis and Test Center.

## Compliance with ethical standards

**Conflicts of interest** The authors declare that they have no conflict of interests.

## References

- Cheong WJ, Yang SH, Ali F. Molecularly imprinted polymers for separation science: a review of reviews. *J Sep Sci.* 2013;36:609–28.
- Martin-Esteban A. Molecularly-imprinted polymers as a versatile, highly selective tool in sample preparation. *Trac-Trend Anal Chem.* 2013;45:169–81.
- Ye L, Mosbach K. Molecular imprinting: synthetic materials as substitutes for biological antibodies and receptors. *Chem Mater.* 2008;20:859–68.
- Ji W, Ma X, Zhang J, Xie H, Liu F, Wang X. Preparation of the high purity gingerols from ginger by dummy molecularly imprinted polymers. *J Chromatogr A.* 2015;1387:24–31.
- Fan W, Gao M, He M, Chen B, Hu B. Cyromazine imprinted polymers for selective stir bar sorptive extraction of melamine in animal feed and milk samples. *Analyst.* 2015;140:4057–67.
- Ye L. Molecularly imprinted polymers with multi-functionality. *Anal Bioanal Chem.* 2016;408:1727–33.
- Wei W, Liang R, Wang Z, Qin W. Hydrophilic molecularly imprinted polymers for selective recognition of polycyclic aromatic hydrocarbons in aqueous media. *RSC Adv.* 2015;5:2659–62.
- You QP, Peng MJ, Zhang YP, Guo JF, Shi SY. Preparation of magnetic dummy molecularly imprinted polymers for selective extraction and analysis of salicylic acid in *Actinidia chinensis*. *Anal Bioanal Chem.* 2014;406:831–9.

9. Chen L, Xu S, Li J. Recent advances in molecular imprinting technology: current status, challenges and highlighted applications. *Chem Soc Rev*. 2011;40:2922–42.
10. Zhao M, Zhang C, Zhang Y, Guo X, Yan H, Zhang H. Efficient synthesis of narrowly dispersed hydrophilic and magnetic molecularly imprinted polymer microspheres with excellent molecular recognition ability in a real biological sample. *Chem Commun*. 2014;50:2208–10.
11. Hao Y, Gao R, Shi L, Liu D, Tang Y, Guo Z. Water-compatible magnetic imprinted nanoparticles served as solid-phase extraction sorbents for selective determination of trace 17 $\beta$ -estradiol in environmental water samples by liquid chromatography. *J Chromatogr A*. 2015;1396:7–16.
12. Zhang H. Water-compatible molecularly imprinted polymers: promising synthetic substitutes for biological receptors. *Polymer*. 2014;55:699–714.
13. Adali-Kaya Z, Bui BTS, Falcimaigne-Cordin A, Haupt K. Molecularly imprinted polymer nanomaterials and nanocomposites: atom-transfer radical polymerization with acidic monomers. *Angew Chem Int Ed*. 2015;54:5192–5.
14. Yan H, Row KH, Yang G. Water-compatible molecularly imprinted polymers for selective extraction of ciprofloxacin from human urine. *Talanta*. 2008;75:227–32.
15. Benito-Pena E, Martins S, Orellana G, Moreno-Bondi MC. Water-compatible molecularly imprinted polymer for the selective recognition of fluoroquinolone antibiotics in biological samples. *Anal Bioanal Chem*. 2009;393:235–45.
16. Yang Y, Long Y, Cao Q, Li K, Liu F. Molecularly imprinted polymer using  $\beta$ -cyclodextrin as functional monomer for the efficient recognition of bilirubin. *Anal Chim Acta*. 2008;606:92–7.
17. Kyaas GZ, Bikiaris DN, Lazaridis NK. Selective separation of basic and reactive dyes by molecularly imprinted polymers (MIPs). *Chem Eng J*. 2009;149:263–72.
18. Yang K, Berg MM, Zhao C, Ye L. One-pot synthesis of hydrophilic molecularly imprinted nanoparticles. *Macromolecules*. 2009;42:8739–46.
19. Puoci F, Lemma F, Cirillo G, Curcio M, Parisi OI, Spizzirri UG, et al. New restricted access materials combined to molecularly imprinted polymers for selective recognition/release in water media. *Eur Polym J*. 2009;45:1634–40.
20. Ji W, Chen L, Ma X, Wang X, Gao Q, Geng Y, et al. Molecularly imprinted polymers with novel functional monomer for selective solid-phase extraction of gastrodin from the aqueous extract of *Gastrodia elata*. *J Chromatogr A*. 2014;1342:1–7.
21. Ji W, Zhang M, Wang D, Wang X, Liu J, Huang L. Superhydrophilic molecularly imprinted polymers based on a water-soluble functional monomer for the recognition of gastrodin in water media. *J Chromatogr A*. 2015;1425:88–96.
22. Boros CA, Stemmitz FR. Iridoids. An updated review. Part I. *J Nat Prod*. 1990;53:1055–147.
23. Boros CA, Stemmitz FR. Iridoids. An updated review. Part II. *J Nat Prod*. 1991;54:1173–246.
24. Chinese Pharmacopoeia Commission, editor. Chinese pharmacopoeia, vol. I. Beijing: People's Medical Publishing House; 2010. p. 26.
25. Chinese Pharmacopoeia Commission, editor. Chinese pharmacopoeia, vol. I. Beijing: People's Medical Publishing House; 2010. p. 597.
26. Song Y, Li SL, Wu MH, Li HJ, Li P. Qualitative and quantitative analysis of iridoid glycosides in the flower buds of *Lonicera* species by capillary high performance liquid chromatography coupled with mass spectrometric detector. *Anal Chim Acta*. 2006;564:211–8.
27. Cao XY, Wang ZZ. Simultaneous determination of four iridoid and secoiridoid glycosides and comparative analysis of *Radix Gentianae macrophyllae* and their related substitutes by HPLC. *Phytochem Anal*. 2010;21:348–54.
28. Yang L, Wang Y, Wang L, Xiao H, Wang Z, Hu Z. Rapid quantification of iridoid glycosides analogues in the formulated Chinese medicine *Longdan Xiegan* Decoction using high-performance liquid chromatography coupled with mass spectrometry. *J Chromatogr A*. 2009;1216:2098–103.
29. He ML, Cheng XW, Chen JK, Zhou TS. Simultaneous determination of five major biologically active ingredients in different parts of *Gardenia jasminoides* fruits by HPLC with diode-array detection. *Chromatographia*. 2006;64:713–7.
30. Bergonzi MC, Righeschi C, Isacchi B, Bilia AR. Identification and quantification of constituents of *Gardenia jasminoides* Ellis (Zhizi) by HPLC-DAD-ESI-MS. *Food Chem*. 2012;134:1199–204.
31. Coran SA, Mulas S, Vasconi A. Profiling of components and validated determination of iridoids in *Gardenia jasminoides* Ellis fruit by a high-performance-thin-layer-chromatography/mass spectrometry approach. *J Chromatogr A*. 2014;1325:221–6.
32. Han Y, Wen J, Zhou T, Fan G. Chemical fingerprinting of *Gardenia jasminoides* Ellis by HPLC-DAD-ESI-MS combined with chemometrics methods. *Food Chem*. 2015;188:648–57.
33. Ji W, Xie H, Zhou J, Wang X, Ma X, Huang L. Water-compatible molecularly imprinted polymers for selective solid phase extraction of dencichine from the aqueous extract of *Panax notoginseng*. *J Chromatogr B*. 2016;1008:225–33.
34. Ji W, Ma X, Xie H, Chen L, Wang X, Zhao H, et al. Molecularly imprinted polymers with synthetic dummy template for simultaneously selective removal and enrichment of ginkgolic acids from *Ginkgo biloba* L. leaves extracts. *J Chromatogr A*. 2014;1368:44–51.
35. Zengina A, Yildirima E, Tamerb U, Caykara T. Molecularly imprinted superparamagnetic iron oxide nanoparticles for rapid enrichment and separation of cholesterol. *Analyst*. 2013;138:7238–45.
36. Zhang L, Wu J, Wang Y, Long Y, Zhao N, Xu J. Combination of bioinspiration: a general route to superhydrophobic particles. *J Am Chem Soc*. 2012;134:9879–81.
37. Lenain P, Mavungu JDD, Dubruel P, Robbens J, Saeger SD. Development of suspension polymerized molecularly imprinted beads with metergoline as template and application in a solid-phase extraction procedure toward ergot alkaloids. *Anal Chem*. 2012;84:10411–8.
38. Software calculated value from SciFinder Scholar database 2008. <http://www.cas.org/products/sfacad/>.